Finger and forehead PPG signal comparison for respiratory rate estimation

A Hernando[1,2,4], M D Peláez-Coca[1,2], M T Lozano[1,2], J Lázaro[2,3,4] and E Gil[2,4].

[1] Centro Universitario de la Defensa (CUD), Academia General Militar (AGM), Zaragoza, Spain.
[2] BSICoS Group, Aragón Institute of Engineering Research (I3A), IIS Aragón, University of Zaragoza, Zaragoza, Spain.
[3] Department of Biomedical Engineering, University of Connecticut, Storrs CT, USA.
[4] Centro de Investigación Biomédica en Red Bioingeniería, Biomateriales y Nanomedicina (CIBER-BBN), Madrid, Spain.

E-mail: ahersanz@unizar.es

Abstract.

Objective: an evaluation of the location of the photoplethysmogram (PPG) sensor for respiratory rate estimation is performed. **Approach:** finger-PPG, forehead-PPG, and respiratory signal were simultaneously recorded from 35 subjects while breathing spontaneously, and during controlled respiration experiments at a constant rate from 0.1 Hz to 0.6 Hz, in 0.1 Hz steps. Four PPG derived respiratory (PDR) signals were extracted from each one of the recorded PPG signals: pulse rate variability (PRV), pulse width variability (PWV), pulse amplitude variability (PAV) and the respiratory-induced intensity variability (RIIV). Respiratory rate was estimated from each one of the 4 PDR signals for both PPG sensor locations. In addition, different combinations of PDR signals, power distribution of the respiratory frequency range and differences of the morphological parameters extracted from both PPG signals have been analysed. **Main results:** results show a better performance in terms of successful estimation and relative error when: i) PPG signal is recorded in the finger; ii) the respiratory rate is less than 0.4 Hz; iii) RIIV signal is not considered. Furthermore, lower spectral power around the respiratory rate in the PDR signals recorded from the forehead was observed. **Significance:** these results suggest that respiratory rate estimation is better at lower rates (0.4 Hz and below) and that finger is better than forehead to estimate respiratory rate.

Keywords: Photoplethysmogram(PPG), finger, forehead, respiratory rate estimation

1. Introduction

Pulse photopletysmographic (PPG) signal is a non-invasive technique widely used to obtain clinic monitoring information (Shelley 2007, Seymour *et al* 2010). This technique was explained for first time (by Hertzman and Spielman 1937) and it was usually used to detect blood volume changes in the microvascular bed of tissue (Challoner 1979). Nowadays, PPG measure needs only one low-cost device widely used in the clinical routine that can be located in several parts of the body. Among its multiple applications, the most highlighted are (Allen 2007): evaluation of the Autonomic Nervous System (ANS), through the Heart Rate Variability (Nitzan *et al* 1998 and Gil *et al* 2010); vascular assessment, measuring the arterial disease, compliance or ageing among others characteristics of the vascular tissue (Takazawa *et al* 1998); and the physiological monitoring of the organism, estimating the heart rate and the oxygen saturation (Chon *et al* 2009 and Jensen *et al* 1998).

Analysis of the pulse photopletysmographic waveform also offers a non-invasive alternative of respiratory rate monitoring based on the assumption that respiration modulates PPG signal through several effects (Meredith *et al* 2012). A lot of works have developed algorithms to estimate respiratory rate from PPG signal directly, as in (Chon *et al* 2009) where respiratory rate is estimated using time-frequency spectral methods or in (Lin *et al* 2013) where autoregressive decomposition is applied. Other works prefer to develop their algorithms over PPG derived respiration (PDR) signals, which reflect the respiratory modulation over the PPG. Probably, the most common PDR signal used to extract the respiratory information is the respiratory-induced intensity variability signal (RIIV) (Nilsson *et al* 2000, Lin *et al* 2013, Karlen *et al* 2013). This modulation arises from respiratory-induced variations in venous return to the heart, caused by the alterations in intrathoracic pressure. Other possible PDR signals described in the literature are: Pulse Rate Variability (PRV), modulated by respiration through respiratory sinus arritmia (Dash *et al* 2010); Pulse Amplitude Variability (PAV), also modulated by respiration through variations in stroke volume and in blood vessels stiffness (Johansson and Oberg 1999); and Pulse Width Variability (PWV), modulated by blood vessels stiffness in addition to the pressure changes in the thorax during respiratory cycle (Lázaro *et al* 2013). Respiratory rate estimation can be done over one of this PDR signals or over an ensemble of them, through the application of several techniques as fusion of fast Fourier transforms (Karlen *et al* 2013), wavelet transform methods (Addison *et al* 2015) or peak-averaged combination of power spectra estimation (Lázaro *et al* 2013).

All the mentioned works have one thing in common: PPG sensor is located in the finger. However, morphological changes in PPG have been observed due to the body location where PPG is registered (Allen 2007, Hartmann *et al* 2019) and due to different respiratory patterns as deep or spontaneous breathing (Hartmann *et al* 2019). Even more, PPG signal spectral power in the respiratory band is also affected by the PPG sensor location (Nilsson *et al* 2007). Few works in the bibliography have compared

respiratory rate estimation extracted from different PPG locations, as in (Johnston and Mendelson 2004) where finger and forehead were compared and good results were obtained in both locations or in (Charlton *et al* 2017) where finger was chosen as the best place to locate the PPG sensor. However, these works do not explore the reasons of why these locations present a different performance. Therefore, we propose one more deep study comparing respiratory rate estimation of two possible PPG sensor locations, together with a power spectral analysis and a PPG morphological study to find out the best place to estimate respiratory rate and its causes.

In this work, PPG signal is recorded in finger and forehead and PRV, PAV, PWV and RIIV signal are extracted from each location. Respiratory rate for these PDR signals (and all the possible combinations of them) is estimated and the success rate, the relative error and a confusion matrix are computed to evaluate how the location of the PPG sensor affects to the respiratory rate estimation. The power distribution of respiratory information and some morphological parameters of both PPG signals are studied too to complete the analysis. A preliminary version of this work was presented (Hernando *et al* 2017), where only finger and forehead respiratory rate estimation from PAV was classified as correct or wrong if matched with the reference, in a subset of 10 subjects.

2. Materials

Thirty-five subjects (18 males and 17 females) with a mean age of 35.1 $\pm$ 6.5 years conformed the whole database. During the whole test subjects remained comfortably seated during approximately half an hour. The protocol consisted of 7 different stages with a duration of 3 minutes each one: first, subjects are registered during spontaneous breathing; then a different respiratory rate is imposed in each of the remaining six stages, starting at 0.6 Hz and ending at 0.1 Hz in steps of 0.1 Hz. This controlled breathing is given by a sinusoidal wave that the subjects had to follow, marking the moment of inhale and exhale.

Finger and forehead PPG signals were recorded simultaneously as well as a chest-band respiratory signal. These signals were registered with the Medicom System, ABP-10 module (Medicom MTD, Ltd, Russia), a device specifically created to acquire raw biomedical signals without any pre-processing. The sample frequency was f_s =250 Hz. Only the last 2 minutes of each stage are used to extract the features of the wave morphology and the respiratory information from the PPG signals. Results of respiratory chest-band signal obtained the same respiratory rate imposed by the guided sinusoidal wave, so it was used as the reference to compare the respiratory rate estimated from finger and forehead PPG.

3. Methods

3.1. PPG derived respiration signals

First of all, a band-pass filter (cut-off frequencies of 0.3-35 Hz) was applied to both PPG signals ($x_{\mathrm{PPG}}(n)$) in order to avoid baseline noise and possible interferences (Garzón-Rey *et al* 2017). Then, artefactual pulses were suppressed by using the artefact detector described in (Gil *et al* 2008). Finally, the apex ($n_{\mathrm{A}i}$), the basal ($n_{\mathrm{B}i}$) and the medium ($n_{\mathrm{M}i}$) points of PPG pulses were automatically detected using an algorithm based on a low-pass differentiator filter (Lázaro *et al* 2014). The medium points are considered the fiducial points in PPG (Peralta *et al* 2019) to compute the pulse to pulse (PP_i) time series. Onset ($n_{\mathrm{O}i}$) and end ($n_{\mathrm{E}i}$) of the pulses were detected as described in (Lázaro *et al* 13). Figure 1 shows an example of finger and forehead signals with their most representative points highlighted.

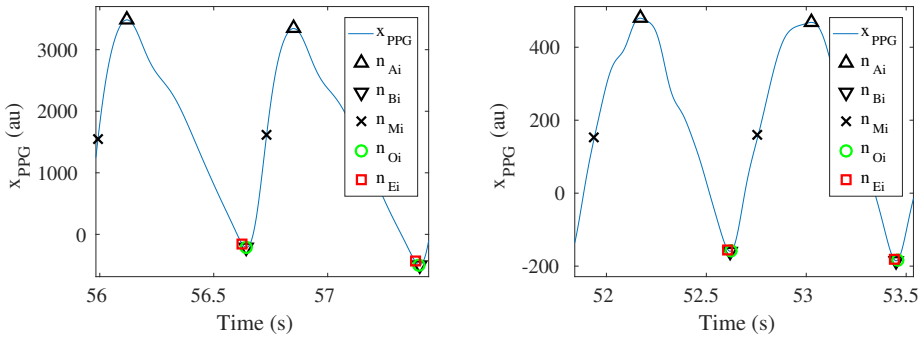

(a) (b)

Figure 1. Two pulse waves of the both PPG signal (left image, finger PPG; right image, forehead PPG; measure in arbitrary units, au) with their most representative points highlighted. Distance between two adjacent medium points is the Pulse to Pulse interval or PP_i, used to compute the time series.

Finally, 4 PDR signals were obtained:

- Pulse Rate Variability (PRV) represents the time difference between two adjacent medium points (Bailón *et al* 2011):

$$d^u_{\mathrm{PRV}}(n) = \sum_i f_s \delta(n - n_{\mathrm{M}i})/(n_{\mathrm{M}i} - n_{\mathrm{M}i-1}). \tag{1}$$

- Pulse Amplitude Variability (PAV) reflects the amplitude variation between the apex and the basal points (Lázaro *et al* 2013):

$$d^u_{\mathrm{PAV}}(n) = \sum_i \left[x_{\mathrm{PPG}}(n_{\mathrm{A}i}) - x_{\mathrm{PPG}}(n_{\mathrm{B}i})\right] \delta(n - n_{\mathrm{M}i}). \tag{2}$$

- Pulse Width Variability (PWV) reflects the width variation of the pulses:

$$d^u_{\mathrm{PWV}}(n) = \sum_i \frac{1}{f_s}(n_{\mathrm{E}i} - n_{\mathrm{O}i})\delta(n - n_{\mathrm{M}i}). \tag{3}$$

- Respiratory-Induced Intensity Variability (RIIV) was estimated from (n_{Bi}) (Karlen *et al* 2013). It must be noticed that for this PDR signal the initial band-pass filter is not applied in order to maintain the intensity variations produced by the respiration.

$$d^{u}_{\mathrm{RIIV}}(n) = \sum_{i} \left[x_{\mathrm{PPG}}(n_{\mathrm{B}i})\right] \delta(n - n_{\mathrm{M}i}). \tag{4}$$

The four PDR signals assume that their variations are due to a modulation based on respiratory information. These signals are unevenly sampled (superscript u) so a resampling at 4 Hz to standardize them is applied using cubic splines in addition to a median-absolute-deviation based outlier rejection rule. Then, a band-pass filter (cut-off frequencies of 0.07-0.8 Hz) is applied over the PDR signals in order to limit the analysis within the frequency range where respiratory information is (Lázaro *et al* 2013). An example of the four PDR signals is shown in Figure 2.

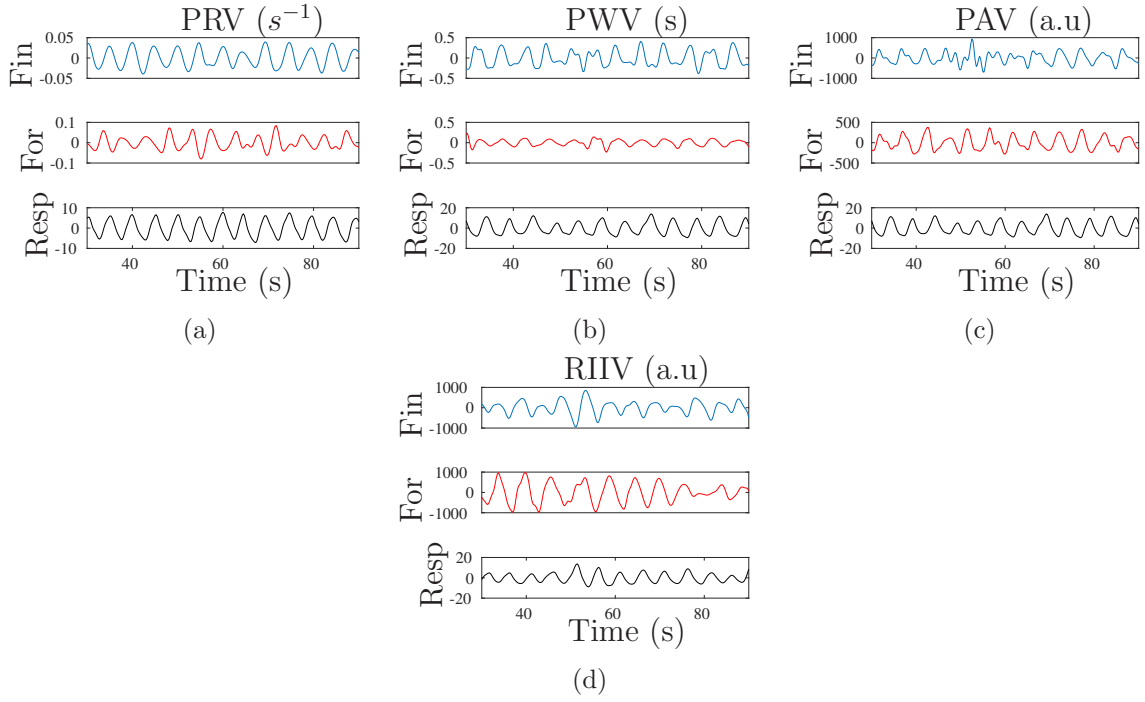

Figure 2. One minute representation of the respiration extracted in the finger (Fin, in blue), in the forehead (For, in red) and the chest-band respiratory signal (Resp, in black) for the 4 PDR signals (PRV, PWV, PAV and RIIV, one each column respectively).

3.2. Respiratory rate estimation

A fusion technique based on frequency analysis of PDR signals (Lázaro *et al* 2013) is applied to estimate respiratory frequency ($\hat{F}_{\mathrm{R}}$) every 5 seconds from "peaked-conditioned" averaged spectra. This method estimates a power spectrum density every 5 seconds from a 40 s length running window of each PDR signal using the Welch's

periodogram. The biggest peak near the previous respiratory rate estimation is selected and the percentage of power around this peak with respect a reference interval is computed. If this percentage is higher than a established threshold (if the signal is peaked enough), it means than respiratory information of this PDR signal is very clear, so this spectrum is promediated together to the other PDR spectra peaked enough and a peaked-conditioned average spectra is obtained. The location of the largest peak in this average spectra is selected as the new respiratory rate estimation. This algorithm can be applied over a single PDR signal or over a combination of them, so results of the estimated respiratory rate using all the possible combination of PDR signals are considered.

The same method is applied over the respiratory chest-band information in order to obtain a reference of the real respiratory rate (F_{C}), that is going to be used as the reference to check every PDR signal and combination performance.

3.3. Performance measurements and PDR signal characteristics

A comparison between the respiratory rate estimated with the PDR signals and from the reference is done every 5 seconds with an experimental margin of error of $\pm$ 0.05 Hz ($\pm$ 0.3 bpm). If the estimation matches with the reference, it is considered as a Correct Estimation (CE), while a Wrong Estimation (WE) is considered otherwise. The success rate is used as a performance measure:

$$SR = CE/(CE + WE) \times 100. \tag{5}$$

The inter-subject mean of this percentage is calculated for every stage and for each PDR signal and all possible combination of them. Also, a confusion matrix was computed to analyse what happen when the respiratory rate was not successfully estimated.

In addition, the relative error (e_{r}) of the respiratory rate estimation is also calculated:

$$e_{\mathrm{r}} = (\hat{F}_{\mathrm{R}} - F_{\mathrm{C}})/F_{\mathrm{C}} \times 100. \tag{6}$$

Another interesting point of study is the power distribution for each PDR signal. Thus, for each stage, the power within a bandwidth of 0.1 Hz around the expected respiratory frequency (given by the respiratory chest-band, F_{C}) is compared with the total power in the spectra (from 0.07 to 0.65 Hz).

$$P_{\mathrm{R}}(k) = (\int_{f=F_{\mathrm{C}}-0.05}^{f=F_{\mathrm{C}}+0.05} \bar{S}_k(f)\, df)/(\int_{f=0.07}^{f=0.65} \bar{S}_k(f)\, df). \tag{7}$$

where $\bar{S}_k(f)$ is the peaked-conditioned average spectra and k represents the time instant (every 5 seconds) (Lázaro *et al* 2013). This ratio aims to quantify how much power related to the respiratory component appears in each PDR signal in each stage, assuming than higher relative power means more respiratory signal-to-noise ratio.

The possible variations between each pair of PDR signals from the finger and the forehead could be due to differences in the wave morphology associated to the location (Allen 2007, Nilsson *et al* 2007). Therefore, the width and the pulse rate are analysed for each pulse of the PPG signal (denoted with the index i) in the finger and the forehead:

- Width: reflects the pulse width of each wave.

$$PW_i = n_{\mathrm{E}i} - n_{\mathrm{O}i} \tag{8}$$

- Rate: reflects the difference between adjacent medium points.

$$PR_i = 1/(n_{\mathrm{M}i} - n_{\mathrm{M}i-1}) \tag{9}$$

Finally, an statistical analysis is made to compare all these results obtained with the PPG signal registered in the finger and the forehead. First, a Shapiro-Wilk test is applied to verify the normal distribution of the data. The t-Student test is applied if the distribution is normal, otherwise, the Wilcoxon paired test is the one applied. In both methods, p-value ≤ 0.05 defines the significance.

4. Results

Figure 3 shows an example of the time-frequency maps ($\bar{S}_k(f)$) of 8 different PDR signals during the controlled breathing stage at a respiratory rate of 0.4 Hz. Each row represents one different PPG signal (finger and forehead) and each column corresponds with one different PDR signal (PRV, PWV, PAV and RIIV). The image shows a high spectral power component (yellow zone) around the expected respiratory rate (red line) in six out of eight PDR signals. In the other two, (RIIV extracted in finger and forehead), the main frequency component is located between 0.1 and 0.2 Hz and no related to respiration.

Table 1 shows the respiratory rate estimation success rate in each stage using a single PDR signal and with all the possible combinations of them, for both possible PPG sensor locations. Results show a better performance of the algorithm at low respiratory rates and when the sensor is located in the finger. When only one PDR signal is used, PRV obtains the best results at lower frequencies but when the frequency is above 0.2 Hz PAV reaches the best results in finger and PWV in forehead. Good results are found when several signals are combined, specially with PRV-PWV, PWV-PAV and PRV-PWV-PAV. The worst results are found with RIIV signal (and all its combinations) except in 0.1 Hz stage. It must be noticed that combining PDR signals does not imply an increase in success rate.

Table 2 shows the relative error of each single PDR signal and with all the possible combinations of them for both possible PPG sensor locations. It must be noticed that the error is usually negative (except in 0.1 Hz stage). This indicates that the estimated respiratory rate is lower than the real respiratory rate. Results show lower error when the sensor is located in the finger and when the respiratory rate is low. Similar to Table 1, the lower error is found in PAV in finger and in PWV in forehead when only

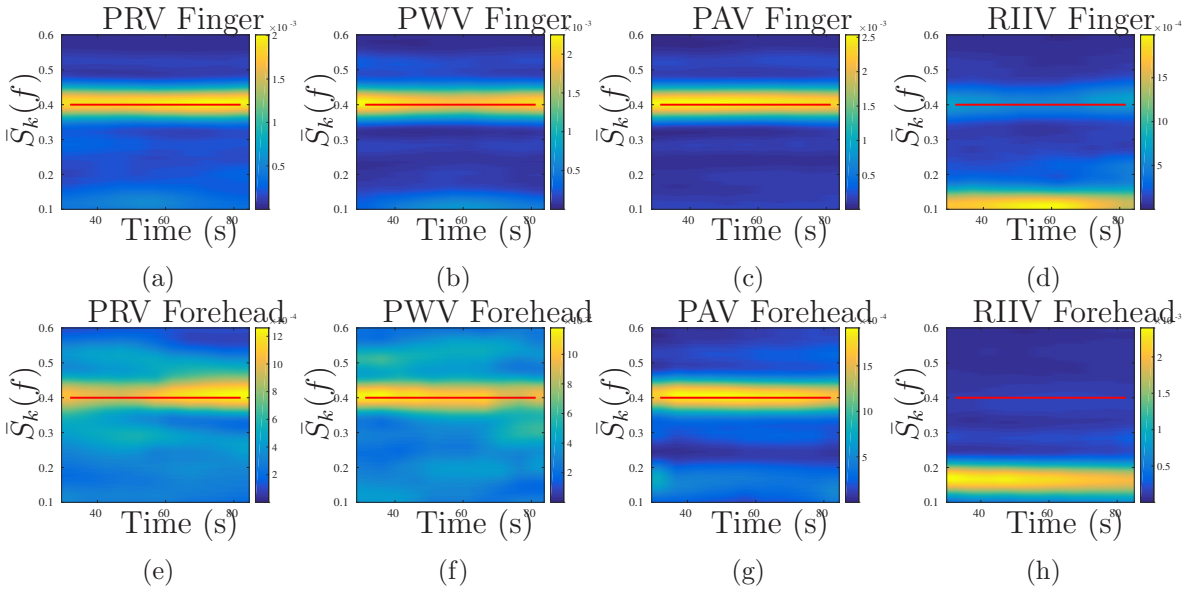

Figure 3. Time-frequency maps of the respiratory rate estimation using the finger (upper row) and the forehead (lower row) PPG signal with different PDR signals separately: a) and e) PRV; b) and f) PAV; c) and g) PWV; d) and h) RIIV. Red line represents the chest-band respiratory rate estimation.

one PDR signal is used. Also, combinations that show a low error are PWV-PAV and PRV-PWV-PAV.

Due to the differences found in the respiratory rate estimation of every PDR signal, a study of the 4 PDR signals separately is done to analyse the causes of the differences between both locations of the PPG sensor. Table 3 shows 4 confusion matrix where all the estimations of each single PDR signal are compared with respect to the reference respiratory rate given by the chest band for both possible PPG sensor locations. Results show higher accuracy in lower frequencies and in finger with respect to forehead estimations. In PRV, PWV and PAV the diagonal presents the highest values (this indicates than the estimation match with the reference) except from 0.6 Hz stage in PRV and PAV. In RIIV, in all the stages except in 0.2 Hz, the highest percentage of estimations is found in the 0.1 Hz stage in finger and in 0.1 and 0.2 Hz stages in forehead. This means that, when an error occurs, the respiratory rate estimation is 0.1 or 0.2 Hz in most of the cases. This result is in agreement with the poor success rate showed in Table 1 and with the large negative error in Table 2.

Figure 4 shows the boxplots of the relative power ($\overline{P_{\mathrm{R}}}$) in normalized units (n.u.). $\overline{P_{\mathrm{R}}}$ in the finger is higher than in the forehead and it decreases when the frequency increases in the four PDR signals. PWV is the one that shows less significant differences in both locations, only in 0.2 and 0.3 Hz stages.

Not only differences in the power distribution have been found. Also morphological differences between the two PPG signals extracted in the finger and the forehead have been noticed. Figure 5 shows the width and rate of the PPG signal in both locations. The width is higher in the forehead than in the finger but the rate remains nearly equal

Table 1. Mean ± std of the respiratory rate estimation success rate (SR) using the PDR signals separately and all the possible combinations of them, in both locations (Fin for finger and For for forehead). Best results of each stage (single, double or triple combination) are highlighted in bold. Significant differences between finger and forehead values are indicated with an $*$ ($p < 0.01$) or with a $**$ ($p < 0.001$).

-	Zone	PRV	PWV	PAV	RIIV	PRV PWV	PRV PAV	PRV RIIV	PWV PAV	PWV RIIV	PAV RIIV	PRV PWV PAV	PRV PWV RIIV	PRV PAV RIIV	PWV PAV RIIV	PRV PWV PAV RIIV
Spt	Fin	70.4± 38.5	69.0± 40.7	**77.1± 40.3**	31.2± 43.5	**76.8± 36.9**	68.3± 40.3	37.4± 43.1	68.8± 39.7	36.6± 42.7	36.1± 42.9	**66.7± 40.9**	37.9± 43.5	37.4± 43.6	36.6± 42.9	37.4± 43.6
	For	51.5± 46.3∗	58.4± 41.8	**63.4± 39.3**	33.8± 42.6	57.5± 45.7∗	60.9± 43.0	37.2± 46.5	**72.5± 36.7**	43.7± 43.4	40.1± 42.8	**59.0± 44.7**	38.5± 46.2	39.0± 46.5	45.0± 43.3	39.2± 46.0
0.1	Fin	**97.4± 15.2**	79.9± 34.4	85.5± 33.5	94.6± 22.4	**97.4± 15.2**	**97.4± 15.2**	**97.4± 15.2**	91.9± 24.6	94.0± 22.5	**97.4± 15.2**	**97.4± 15.2**	**97.4± 15.2**	**97.4± 15.2**	**97.4± 15.2**	97.4± 15.2
	For	**97.1± 14.1**	76.2± 38.6	43.6± 43.4∗∗	78.7± 38.8	94.5± 20.5	**97.1± 14.1**	95.3± 17.4	65.2± 42.0∗	86.8± 26.3	78.4± 38.9∗	**97.1± 14.1**	95.6± 16.5	95.3± 17.4	87.6± 26.7∗	95.6± 16.5
0.2	Fin	**91.0± 25.9**	90.0± 26.2	86.3± 30.9	56.5± 45.0	89.0± 28.1	90.0± 26.9	64.7± 44.6	**91.1± 24.4**	57.5± 44.7	57.1± 46.5	**87.4± 30.0**	63.8± 43.8	62.3± 45.2	56.0± 45.9	61.4± 44.5
	For	**77.3± 32.8**	76.6± 35.1	54.9± 44.4∗	59.8± 44.4	**80.1± 31.8**	69.1± 38.5∗	59.2± 44.9	70.1± 39.8∗	65.2± 41.6	59.3± 43.4	**75.1± 36.0**	56.0± 45.7	58.9± 44.6	64.3± 43.0	56.0± 45.7
0.3	Fin	83.1± 34.2	77.7± 38.0	**89.3± 24.7**	30.6± 44.1	81.8± 37.1	82.1± 35.5	43.5± 45.8	**86.8± 31.4**	39.7± 45.0	38.2± 47.1	**80.0± 37.4**	46.3± 45.3	44.9± 46.1	41.3± 45.9	45.4 45.9
	For	58.0± 45.0∗∗	**72.4± 39.5**	63.3± 46.7∗	2.9± 16.9∗∗	64.5± 42.1∗	63.7± 41.0	10.1± 24.5∗∗	**73.4± 37.9**	12.4± 29.3∗∗	15.4± 30.8∗	**63.6± 41.7**	12.6± 27.5∗∗	15.7± 28.7∗∗	18.6± 33.3∗	16.2± 30.7∗∗
0.4	Fin	68.3± 45.8	58.7± 46.9	**78.6± 39.4**	30.4± 45.9	58.4± 48.2	**66.0± 46.4**	35.9± 45.2	61.2± 43.8	26.0± 43.3	39.0± 44.5	**57.4± 47.3**	29.1± 44.0	38.3± 44.0	28.6± 42.4	28.6± 42.4
	For	45.1± 47.4	**60.0± 42.7**	55.1± 43.6∗	1.3± 7.7∗∗	**54.0± 46.9**	44.9± 46.1∗	2.6± 13.9∗∗	51.6± 44.3	8.3± 23.8∗	5.3± 17.2∗∗	**44.6± 46.0**	4.7± 17.4∗	4.2± 15.2∗∗	9.6± 23.4∗	5.7± 18.2∗
0.5	Fin	57.7± 49.6	51.1± 47.3	**75.8± 40.7**	17.4± 36.5	53.9± 48.8	57.4± 49.1	17.4± 36.5	**61.3± 45.1**	17.9± 36.9	21.8± 38.8	**55.8± 47.6**	17.7± 36.8	20.3± 38.5	22.1± 39.5	20.0± 38.6
	For	40.0± 41.3	**45.2± 46.5**	40.3± 47.2∗	0.0± 0.0∗	37.4± 44.2	**40.2± 43.7**	2.9± 16.9∗	37.8± 46.1∗	0.0± 0.0∗	3.9± 16.4∗	**33.7± 42.3**	1.8± 10.7∗	2.9± 16.9∗	1.6± 9.2∗	1.8± 10.8∗
0.6	Fin	36.4± 47.2	45.4± 48.7	**46.5± 48.0**	10.1± 29.4	32.2± 45.9	34.0± 46.3	8.6± 28.4	**43.4± 46.2**	8.6± 28.4	8.6± 28.4	**34.0± 46.3**	8.6± 28.4	8.6± 28.4	8.6± 28.4	8.6± 28.4
	For	27.8± 41.4	**33.5± 45.3**	20.5± 37.0∗	0.0± 0.0	**26.5± 42.7**	15.3± 31.3	0.8± 3.4	14.5± 32.0∗∗	0.8± 4.6	1.8± 8.2	**17.9± 33.5**	0.0± 0.0	0.8± 3.4	1.6± 6.8	0.5± 3.1

for both signals.

5. Discussion

In this paper, an evaluation of how the location of the PPG sensor affects the respiratory rate estimation and which PDR signals are more appropriated to this purpose has been performed. PPG signals were recorded in finger and forehead from subjects breathing spontaneously and at different controlled respiratory rates. 4 PDR technique were applied to both locations of the PPG signals, obtaining one respiratory rate estimation per PDR signal. In addition, respiratory rate was also estimated from all the possible combinations of these 4 PDR techniques. The estimations were compared with the respiratory rate estimated from chest-band, which was taken as reference. A respiratory estimation was considered to be accurate if it differs less than 0.05 Hz (0.3 bpm) from the reference, based on the errors reported in the PDR methods (Lázaro *et al* 2013). The success rate and the relative error of the estimated respiratory rate from both locations are presented, as well as a confusion matrix for each PDR signal to evaluate

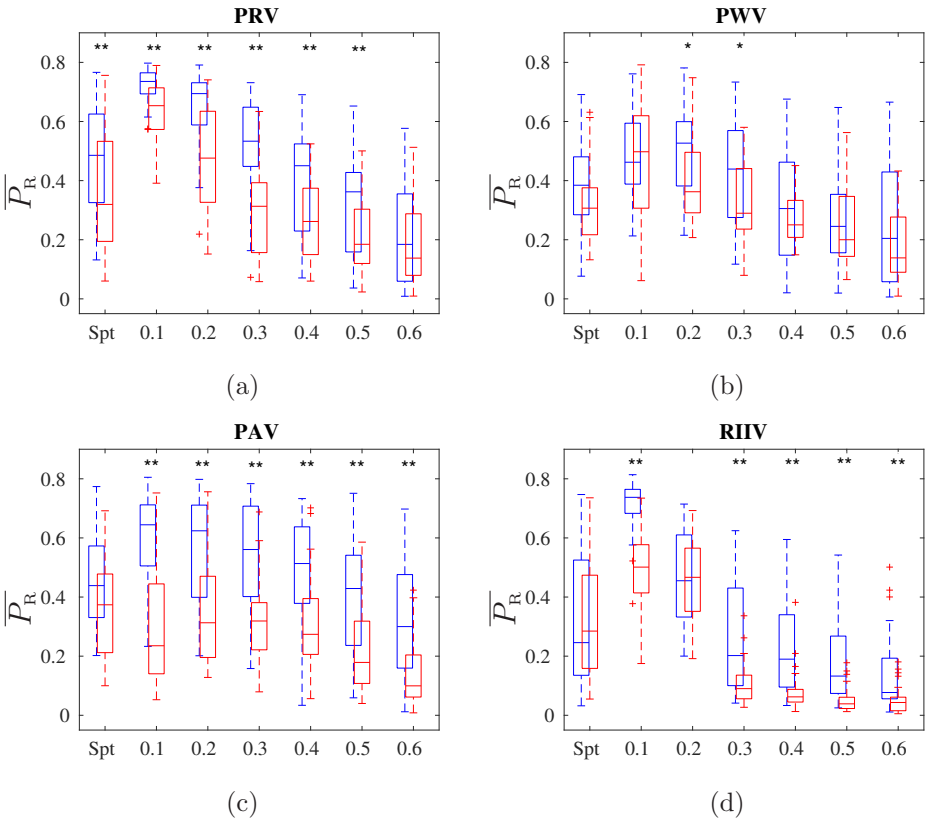

Figure 4. Boxplots of $\overline{P_R}$ from finger (blue) and forehead (red) PPG using a single PDR signal: a) PRV; b) PWV; c) PAV; d) RIIV. Significant differences between finger and forehead values are indicated with an $*$ ($p < 0.01$) or with a $**$ ($p < 0.001$).

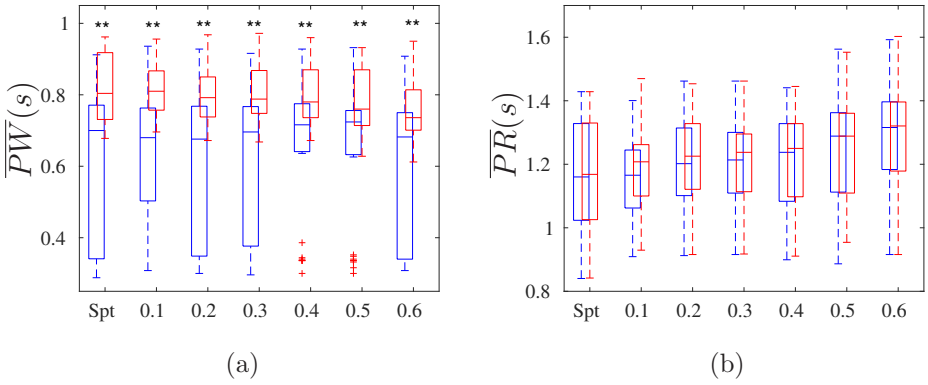

Figure 5. Boxplots of the morphological parameters extracted from finger (blue) and forehead (red) PPG signal. Significant differences between finger and forehead values are indicated with an $*$ ($p < 0.01$) or with a $**$ ($p < 0.001$).

Table 2. Mean ± std of the percentage of the relative error (e_r) committed in the respiratory rate estimation by each PDR signal separately and with all the possible combinations of them, in both locations (Fin for finger and For for forehead). Best results of each stage (single, double or triple combination) are highlighted in bold. Significant differences between finger and forehead values are indicated with an $*$ ($p < 0.01$) or with a $**$ ($p < 0.001$).

-	Zone	PRV	PWV	PAV	RIIV	PRV PWV	PRV PAV	PRV RIIV	PWV PAV	PWV RIIV	PAV RIIV	PRV PWV PAV	PRV PWV RIIV	PRV PAV RIIV	PWV PAV RIIV	PRV PWV PAV RIIV
Spt	Fin	-17.3± 22.3	**-8.2± 27.9**	-9.3± 19.1	-40.4± 23.7	**-14.7± 22.3**	-17.5± 22.2	-36.8± 23.5	-15.2± 21.2	-36.7± 23.6	-37.4± 23.3	**-17.6± 22.6**	-36.5± 23.7	-36.7± 23.7	-37.2± 23.3	-36.7± 23.7
	For	-21.8± 34.0	**1.9± 43.3**	17.0± 41.4	-29.3± 24.1**	-23.5± 23.7	-20.0± 23.7	-33.6± 23.0	**2.7± 34.9***	-24.4± 23.0*	-22.7± 28.7**	**-20.3± 25.2**	-32.6± 22.3	-32.7± 22.0	-24.6± 21.9**	-32.4± 22.1
0.1	Fin	**-1.1± 7.7**	14.8± 30.1	11.3± 33.6	1.3± 16.8	**-1.1± 7.7**	-1.3± 7.6	-1.9± 7.5	3.3± 18.9	1.6± 16.9	-1.5± 7.7	**-1.4± 7.6**	-1.9± 7.5	-1.9± 7.5	-1.5± 7.7	-2.0± 7.5
	For	**0.4± 8.8**	34.8± 72.3*	94.4± 95.7**	19.2± 27.1**	2.3± 14.7	**0.9± 9.3**	1.6± 11.3	56.5± 87.3**	8.4± 18.1*	19.2± 27.3**	**0.8± 9.3**	1.4± 11.0	1.6± 11.3	8.4± 19.0**	1.4± 11.0
0.2	Fin	-4.3± 11.6	-4.6± 10.8	**-1.6± 15.4**	-20.4± 20.6	-5.5± 12.9	-4.9± 12.4	-16.9± 20.6	**-4.5± 11.4**	-20.1± 20.4	-20.2± 21.3	**-6.4± 13.9**	-17.4± 20.3	-18.0± 21.0	-20.8± 20.9	-18.5± 20.6
	For	**-4.2± 22.6**	6.3± 19.8*	31.4± 50.4**	-19.6± 16.0	-7.4± 15.5	**2.2± 33.4**	-20.4± 15.5	16.2± 32.2*	-13.8± 18.6	-12.7± 24.4	**-4.2± 23.4**	-17.9± 22.9	-20.2± 15.7	-12.9± 22.7	-17.9± 22.9
0.3	Fin	-9.8± 20.9	-10.5± 20.7	**-5.5± 14.3**	-42.6± 28.4	-10.9± 22.5	-10.3± 21.3	-34.4± 28.7	**-7.6± 18.4**	-36.7± 28.4	-38.2± 29.6	**-11.8± 22.3**	-32.7± 28.6	-33.7± 29.2	-35.9± 28.7	-33.4± 29.0
	For	-18.3± 28.6	**-7.3± 21.3**	-10.8± 25.5	-49.1± 11.2	-14.3± 28.2	-18.6± 23.0	-46.7± 16.5*	**-12.6± 20.2**	-44.6± 17.0	-41.7± 18.0	**-19.5± 23.7**	-46.5± 16.3*	-44.5± 17.3	-41.0± 18.9	-44.7± 18.4
0.4	Fin	-22.6± 32.7	-24.1± 28.7	**-15.4± 28.2**	-50.2± 33.5	-27.9± 33.3	**-24.2± 33.5**	-45.2± 32.8	-24.9± 30.1	-51.4± 31.4	-43.0± 32.8	**-29.2± 33.7**	-49.4± 31.8	-43.7± 32.5	-49.8± 31.0	-49.7± 30.9
	For	-34.6± 32.1	**-17.3± 20.7**	-22.3± 27.4	-62.7± 7.3	-28.6± 30.7	-32.2± 28.9	-61.5± 10.5*	**-24.4± 25.7**	-57.3± 15.7	-58.7± 14.0*	**-32.4± 28.3**	-60.4± 12.4	-60.4± 11.6*	-56.1± 16.7	-59.5± 13.3
0.5	Fin	-30.6± 37.1	-29.9± 31.7	**-16.4± 29.5**	63.9± 28.7	-34.1± 37.1	-31.3± 37.0	-64.0± 28.6	**-25.0± 31.1**	-61.9± 29.4	-59.7± 30.8	**-31.5± 35.5**	-63.4± 28.8	-61.4± 30.3	-58.8± 31.0	-61.5± 30.3
	For	-35.5± 31.5	**-30.7± 29.8**	-31.0± 27.5*	-70.3± 4.4	-37.3± 31.8	-35.3± 30.3	-69.1± 12.8	**-34.4± 29.4**	-69.7± 5.2	-65.6± 14.0	**-39.1± 29.6**	-68.9± 9.5	-67.9± 13.1	-67.7± 10.1	-68.5± 9.7
0.6	Fin	-44.3± 36.1	-36.6± 34.8	**-28.6± 31.7**	-70.7± 25.8	-51.1± 37.3	-43.9± 35.7	-72.4± 23.7	**-37.4± 34.7**	-71.8± 24.0	-72.1± 23.9	**-49.6± 37.2**	-72.8± 23.6	-72.3± 23.8	-72.5± 23.8	-72.5± 23.9
	For	-45.1± 33.5	**-40.1± 31.9**	-45.7± 28.5*	-75.2± 4.1	**-47.9± 33.0**	-55.0± 26.6	-74.0± 8.9	-54.4± 25.8*	-73.7± 9.6	-72.4± 9.9	**-54.9± 27.7**	-74.3± 7.9	-72.6± 12.2	-72.3± 11.0	-74.1± 8.2

their performance. Also, the power distribution of the respiratory information and the rate and the width of both different PPG signals are analysed trying to explain the differences between both sensor locations.

Focus on finger and forehead, since they are the most extended locations of PPG sensor, it can be seen that a change in the place where PPG signal is registered involves other variations that should be considered: different locations imply different configurations in signal acquisition (Allen 2007), as light-transmission configuration can be used in the finger but not in the forehead, where light-reflection is the only possible configuration; the optical features of the skin are not the same in the finger than in the forehead; also the peripheral blood flow varies from one location to another because different capillary vessels irrigate the different zones. These changes affect the PPG morphology, obtaining a smoother waveform when the signal is recorded in forehead than in finger (Allen 2007, Nilsson *et al* 2007). Our hypothesis supposes that this change in the waveform may affect PDR signals, with a decrease in the modulation that respiration induces over these signals. As the same PDR signal is different depending on

Table 3. Confusion matrix by each PDR signal comparing each respiratory rate estimation (vertical axis) with the reference given by the chest band (horizontal axis), in both locations (Fin for finger and For for forehead). Best results of each stage are highlighted in bold.

PRV	Zone	Spt	0.1	0.2	0.3	0.4	0.5	0.6
Spt	Fin	**267**	0	0	0	0	0	0
	For	**196**	0	0	0	0	0	0
0.1	Fin	91	**371**	34	55	119	144	**177**
	For	152	**377**	65	114	150	125	**147**
0.2	Fin	18	0	**348**	8	0	5	11
	For	12	2	**292**	19	18	24	32
0.3	Fin	1	0	0	**317**	2	4	16
	For	1	0	9	**220**	30	22	13
0.4	Fin	2	0	0	0	**259**	8	11
	For	14	0	9	24	**174**	49	39
0.5	Fin	0	0	0	0	0	**220**	26
	For	2	0	1	3	0	**152**	39
0.6	Fin	0	0	0	0	0	0	140
	For	0	0	0	0	0	2	107

PWV	Zone	Spt	0.1	0.2	0.3	0.4	0.5	0.6
Spt	Fin	**262**	0	0	0	0	0	0
	For	**221**	0	0	0	0	0	0
0.1	Fin	75	**305**	34	48	90	88	98
	For	55	**301**	27	41	44	72	101
0.2	Fin	17	66	**346**	30	34	45	56
	For	45	32	**289**	40	18	41	51
0.3	Fin	21	0	2	**298**	30	36	20
	For	38	36	42	**276**	86	63	35
0.4	Fin	4	0	0	4	**226**	18	29
	For	2	6	18	21	**224**	26	23
0.5	Fin	0	0	0	0	0	**194**	3
	For	5	4	0	2	0	**172**	38
0.6	Fin	0	0	0	0	0	0	**175**
	For	11	0	0	0	0	0	**129**

PAV	Zone	Spt	0.1	0.2	0.3	0.4	0.5	0.6
Spt	Fin	**291**	0	0	0	0	0	0
	For	**243**	0	0	0	0	0	0
0.1	Fin	84	**326**	40	30	79	74	92
	For	5	**169**	19	45	65	34	63
0.2	Fin	0	38	**330**	11	0	0	7
	For	35	89	**208**	64	64	100	**119**
0.3	Fin	2	7	2	**339**	3	0	24
	For	26	41	42	**240**	22	47	30
0.4	Fin	2	0	10	0	**298**	17	18
	For	60	76	83	27	**214**	45	48
0.5	Fin	0	0	0	0	0	**290**	60
	For	6	4	22	4	7	**148**	39
0.6	Fin	0	0	0	0	0	0	**180**
	For	2	0	2	0	0	0	78

RIIV	Zone	Spt	0.1	0.2	0.3	0.4	0.5	0.6
Spt	Fin	117	0	0	0	0	0	0
	For	130	0	0	0	0	0	0
0.1	Fin	**255**	**361**	166	**254**	**264**	**310**	**320**
	For	**162**	**298**	145	**198**	**203**	**192**	**203**
0.2	Fin	17	10	**216**	10	1	2	0
	For	79	81	**229**	171	163	182	172
0.3	Fin	0	0	0	116	1	0	13
	For	6	0	0	11	1	0	1
0.4	Fin	0	0	0	0	114	2	7
	For	0	0	2	0	5	0	0
0.5	Fin	0	0	0	0	0	67	1
	For	0	0	0	0	0	0	1
0.6	Fin	0	0	0	0	0	0	40
	For	0	0	0	0	0	0	0

the PPG sensor location, respiratory rate estimation could be affected by this variable. In fact, an important conclusion of this study is that respiratory rate estimation is more accurate when PPG signal is recorded in the finger than in the forehead. The success rate is higher and the relative error is lower in finger than in forehead for all the stages and all the PDR signals. In addition, the diagonal of the confusion matrix shows higher number of correct estimations in finger than in forehead. The fact that respiratory rate estimation is more accurate in finger than in forehead is also reported (Charlton *et al* 2017).

One possible explanation of this best results in finger lies in the relative power of the respiratory band normalized to the entire spectra, represented in Figure 4, where recordings in finger show a higher $\overline{P_{\mathrm{R}}}$ than in the forehead. A higher $\overline{P_{\mathrm{R}}}$ means that the respiratory component is easier to be identified, and therefore, the respiratory rate

estimator has more chances to give a correct result. On the other hand, with a lower value of $\overline{P_{\mathrm{R}}}$ is easier to mislead the respiratory component and consequently getting a wrong estimation. This result is in contrast with (Nilsson *et al* 2007), where the frequency component analysis shows lower power of the respiratory component in the finger compared to other sensor locations. However, our results shows the opposite (see Figure 4) indicating a minor respiratory related component in the forehead mainly at high frequency rates. It is worth noting that signals are recorded in supine position where parasympathetic activity is enhanced and the methodology used is based in the analysis of the PPG signal spectrum (Nilsson *et al* 2007), while our recordings are in sitting position and the analysed spectral power is extracted from PDR signals. Therefore the counterbalance of respiratory related and unrelated components of PDR signals seems to be essential, at least for frequency based methods.

Concerning which PDR signal is the best to estimate the respiratory rate, PRV showed the best results for lower frequencies (below 0.3 Hz), with the higher success rate, the lower relative error and the higher number of correct estimations. However, its performance is not so good for higher frequencies. Above 0.3 Hz, PAV was the one with the best results when PPG is registered in finger, although results in lower frequencies are quite acceptable too. However, PAV shows not so good results in forehead, in fact significant differences have been found in the success rate and the power around the respiratory component between both locations. These bad results of PAV in forehead has been already noticed in our preliminary study (Hernando *et al* 2017), but in that work the preliminary filter to remove the baseline noise was not applied and the obtained results were worse. As other work suggests (Sun *et al* 2019), removing the baseline modulation increases the success rate of PAV signal in forehead (if not, results were as worse as RIIV forehead ones), although its performance is not as good as in the finger. On the other hand, PWV is the one with best results in the forehead, specially in frequencies above 0.3 Hz. PWV is the only PDR signal whose results in finger are quite similar to the forehead ones. This could be explained by the similar distribution of the power related to the respiratory component in both locations, with no significant differences between both sites. The good performance of PRV, PWV and PAV have already been noticed in (Dash *et al* 2010, Lázaro *et al* 2013). RIIV, although it is a very common PDR signal used in many studies (Nilsson *et al* 2000, Karlen *et al* 2013, Lin *et al* 2013), is the one which obtained the worst results. However, it must be highlighted that, in these studies subjects were breathing spontaneously and none of them had studied RIIV signal registered in the forehead. The worst result with RIIV could be explained by the spectral component non-related to respiration previously explained. It must be noticed that this 4 PDR signals have been studied in this specific database, conformed by healthy subjects with a mean age of 35.1 ± 6.5 years. However, in the study of a different database with different subjects, maybe some of these PDR signals could be eliminated as they could not provide faithful respiratory information. For example, while in this database PAV seems to be the one with the best performance, in a different database conformed by patients with a fluid overload PAV may not provide

valid information (Javed et al 2010). Otherwise, in an elderly database where respiratory sinus arrhythmia will be not so significant (De Meersman 1993), PRV performance should decrease. Therefore, the inclusion of each PDR signal in the respiratory rate estimation method should be considered depending on the final application. Finally, the combination of PDR signals does not give the method more robustness, even more, results with a combination of PDR signals are worse in the higher frequency stages. This result is in contrast with the conclusion extracted in several works (Karlen *et al* 2013, Lázaro *et al* 2013), where the PDR signal combination offers more accurate estimations.

Another important conclusion of this work is the best performance of the respiratory estimation in lower frequencies than in higher ones. As Table 1 shows, the success rate decreases 30% from 0.2 to 0.5 Hz stages in almost all the PDR signals (except in PAV) and for both body locations. Consequently, the error committed is higher in 0.5 Hz stage (more than a 25% with respect the 0.2 Hz stage). Spontaneous respiratory stage also shows good results because respiratory rate during rest usually is in the lower frequencies range, with a mean value of 0.23 Hz in this database. The relative error in spontaneous breathing is slightly higher than in 0.3 Hz stage because 6 subjects have a respiratory rate above 0.3 Hz, being more difficult to properly estimate respiratory rate in these cases. The best performance of the respiratory estimation in lower frequencies than in higher ones has also been reported in other studies (Johnston and Mendelson 2004, Addison *et al* 2015, Charlton *et al* 2017). Figure 4 shows less respiratory relative power as the respiratory rate increases, for the 4 PDR signals. Respiratory rate is the only difference in the setup of the different stages, so we interpret that the lower relative power is due to less powerful respiration-related modulation. In case of PRV, this is coherent with the well-known decrease of respiratory sinus arrhythmia as respiratory rate increases (Hirsch and Bishop 1981). A possible reason of this observation is that autonomic nervous system may act as a physiological low-pass filter. That would explain also the effect in PAV and PWV. However, PRV and PWV are affected also by the mechanical effect of respiration on the intrathoracic blood pressure, which may have also a low-pass behaviour (Lázaro *et al* 2014b).

The decrease of the power of the respiratory spectral component at high breathing rates causes that other spectral components non-related with respiration become relevant and act as a confound. Our results suggest the presence of a non-respiratory related spectral component around 0.1 and 0.2 Hz (see Figure 3, specially in RIIV). When an error occurs, respiratory rate estimation based on PDR is usually around 0.15 Hz. In fact, in Table 3 the higher values of the confusion matrix are found either in the expected stage or in 0.1-0.2 Hz. This component, probably related to Mayer waves, and the problems that may cause for respiratory rate estimation has been pointed out in others works (Karlen *et al* 2013), and could significantly influence PPG signal in forehead (Pfurtscheller *et al* 2018). If the respiratory rate of one specific application is expected to be higher than 0.15 Hz, a more restrictive filter with a higher value of the low cut-off frequency could be applied trying to overcome this non-respiratory related component. In this work, a trial with 0.15 Hz as the low cut-off frequency of the filter

that isolate respiratory components has been implemented and results show an increase higher than 20% in the success rate for all the single PDR signals when the PPG is registered in the finger and an increase of 10% in the forehead.

An analysis of the morphology of PPG waveform is also presented in order to study how different the finger and forehead waves are, and whether PPG morphology is affected by the respiratory rate or not. Results show higher width when the PPG is registered in the forehead in comparison with the finger, independently of the respiratory rate. These differences imply morphological changes between both locations, as other studies in the bibliography shown (Allen 2017, Nilsson *et al* 2007). However, the results do not show that these morphological changes cause restrictions in the respiratory rate estimation. In the case of the width of the pulses, a higher width does not imply a decrease in the modulation that the respiration induces over the PWV signal. Therefore, respiratory rate estimation is apparently more affected by the ratio between the respiratory power with respect to the entire spectra that could mask the respiratory information than by morphological factors.

6. Conclusion

It has been shown that differences in the respiratory rate estimation and changes in morphological features are found when the PPG signal is recorded in the finger and in the forehead. General results for respiratory rate estimation are characterized by a better performance in the low frequencies and when the sensor is located in the finger when compared to the forehead. Also, RIIV showed a poor performance and it affected negatively to the accuracy of the estimation when RIIV was combined with other PDR signals. Therefore, finger is the recommended location for PPG signal acquisition and RIIV signal is not recommended, specially when respiratory rate could increase to higher values. For this specific database, although PRV in finger obtain good results in lower frequencies, the use of PAV in finger would be preferable because it also obtains good results at lower frequencies (above 85% of success rate at 0.1 and 0.2 Hz) and the best results at higher frequencies (almost 90% of success rate at 0.3 Hz and above 75% at 0.4 and 0.5 Hz) and during spontaneous breathing (almost 80% of success rate). The inclusion of each PDR signal in the fusion algorithm should be analysed for each specific application considering both the subject population and the breathing pattern, taking into account the effect of these factors on the respiratory modulation of the PPG.

Acknowledgements

This work has been partially financed by Ministerio de Economía, Industria y Competitividad (MINECO) and by fondos FEDER through the project PGC2018-095936-B-I00 and RTI2018-097723-B-I00; and by Centro Universitario de la Defensa (CUD) under the projects CUD2018-08 and UZCUD2017-TEC-04. This work has never been realized without the collaboration of all the volunteers (special mention to the CUD

faculty) and the support of Gobierno de Aragón (Reference Group BSICoS T39-17R) cofunded by FEDER 2014-2020. This project has received funding from the European Unions Framework Programme for Research and Innovation Horizon 2020 (2014-2020) under the Marie Skłodowska-Curie Grant Agreement No. 745755. The computation was performed by the ICTS NANBIOSIS, specifically by the High Performance Computing Unit of CIBER-BBN at University of Zaragoza.

References

Shelley K H 2007 Photoplethysmography: beyond the calculation of arterial oxygen saturation and heart rate *Anesthesia & Analgesia* **105(6)** S31–6.

Seymour C W, Khan J M, Cooke C R, Watkins T R, Heckbert S R and Tea T D 2010 Prediction of critical illness during out-of-hospital emergency care *JAMA* **304** 747–54.

Hertzman A B and Spielman C 1937 Observations on the finger volume pulse recorded photoelectrically *Am. J. Physiol.* **119** 334–5.

Challoner A V 1979 Photoelectric plethysmography for estimating cutaneous blood flow *Non-Inv. Physiol. Meas.* **1** 125–51.

Allen J 2007 Photoplethysmography and its application in clinical physiological measurement *Physiol. Meas.* **28(3)** R1–39.

Nitzan M, Babchenko A, Khanokh B and Landau D 1998 The variability of the photoplethysmographic signal – a potential method for the evaluation of the autonomic nervous system *Physiol. Meas.* **19** 93–102.

Gil E, Orini M, Bailón R, Vergara J M, Mainardi L and Laguna P 2010 Photoplethysmography pulse rate variability as a surrogate measurement of heart rate variability during non-stationary conditions *Physiol. Meas.* **31(9)** 1271–90.

Takazawa K, Tanaka N, Fujita M, Matsuoka O, Saiki T, Aikawa M, Tamura S and Ibukiyama C 1998 Assessment of vasoactive agents and vascular ageing by the second derivative of photoplethysmogram waveform *Hypertension* **32(2)** 365–70.

Chon K H, Dash S and Ju K 2009 Estimation of respiratory rate from photoplethysmogram data using time-frequency spectral estimation *IEEE Trans. Biomed. Eng.* **56(8)** 2054–63.

Jensen L A, Onyskiw J E and Prasad N G N 1998 Meta-analysis of arterial oxygen saturation monitoring by pulse oximetry in adults *Heart & Lung: The Journal of Acute and Critical Care* **27(6)** 387–408.

Meredith D J, Clifton D, Charlton P, Brooks J, Pugh C W and Tarassenko L 2012 Photoplethysmographic derivation of respiratory rate: a review of relevant physiology *J. Med. Eng. Technol.* **36(1)** 1–7.

Lin Y D, Ho H Y, Tsai C C, Wang S F, Lin K P and Chang H H 2013 Simultaneous heartbeat and respiration monitoring using PPG and RIIV on a smaprtphone device *Biomed. Eng. App. Basis Com.* **25(04)** 135–41.

Nilsson L, Johansson A and Kalman S 2000 Monitoring of respiratory rate in postoperative care using a new photoplethysmographic technique *J. Clin. Monit.* **16** 309–15.

Karlen W, Raman S, Ansermino J M and Dumont G A 2013 Multiparameter Respiratory Rate Estimation From the Photoplethysmogram *IEEE Trans. Biomed. Eng.* **60(7)** 1946–53.

Dash S, Shelley K H, Silverman D G and Chon K H 2010 Estimation of respiratory rate from ECG, photoplethysmogram, and piezo-electric pulse transducer signals: a comparative study of timefrequency methods *IEEE Trans Biomed Eng* **57(5)** 1099–107.

Johansson A and Oberg P A 1999 Estimation of respiratory volumes from the photoplethysmographic signal. Part I: experimental results *Med Biol Eng Comput* **37** 42–7.

Lázaro J, Gil E, Bailón R, Mincholé A and Laguna P 2013 Deriving respiration from photoplethysmographic pulse width *Med. Biol. Eng. Comput.* **51** 233–42.

Addison P S, Watson J N, Mestek M L, Ochs J P, Uribe A A and Bergese S D 2015 Pulse oximetry-derived respiratory rate in general care floor patients *J. Clin. Monit. Comput.* **29(1)** 113–20.

Hartmann V, Liu H, Chen F, Qiu Q, Hughes S and Zhenq D 2019 Quantitative Comparison of Photoplethysmographic Waveform Characteristics: Effect of Measurement Site *Front. Physiol.* **10** 198–205.

Nilsson L, Goscinski T, Kalman S, Lindberg L G and Johansson A 2007 Combined photoplethysmographic monitoring of respiration rate and pulse: a comparison between different measurement sites in spontaneously breathing subjects *Acta Anaesthesiologica Scandinavica* **51** 1250–7.

Johnston W S and Mendelson Y 2004 Extracting breathing rate information from a wearable reflectance pulse oximeter sensor *IEEE Engineering in Medicine and Biology Society* **2** 5388–91.

Charlton P H, Bonnici T, Tarassenko L, Alastruey J, Clifton D A, Beale R and Watkinson P J 2017 Extraction of respiratory signals from the electrocardiogram and photoplethysmogram: technical and physiological determinants *Physiol. Meas.* **38(5)** 669–90.

Hernando A, Peláez-Coca M D, Lozano M T, Aiger M, Gil E and Lázaro J 2017 Finger and forehead PPG signal comparison for respiratory rate estimation based on pulse amplitude variability *25th European Signal Processing Conference (EUSIPCO) Kos (Greece)* 2076–80.

Garzón-Rey J M, Lázaro J, Milagro J, Gil E, Aguiló J and Bailón R 2017 Respiration-Guided Analysis of Pulse and Heart Rate Variabilities for Acute Emotional Stress Assessment *Proc. XLIV Int. Conf. Comp. Card.* 1–4.

Gil E, Vergara J M and Laguna P 2008 Detection of decreases in the amplitude fluctuation of pulse photoplethysmography signal as indication of obstructive sleep apnea syndrome in children *Biomed. Signal Process. Control* **3(3)** 267–77.

Lázaro J, Alcaine A, Romero D, Gil E, Laguna P, Pueyo E and Bailón R 2014 Electrocardiogram Derived Respiratory Rate from QRS Slopes and R-Wave Angle *Annals Biomed. Eng.* **40(10)** 2072–83.

Peralta E, Lázaro J, Bailón R, Marozas V and Gil E 2019 Optimal Fiducial Points for Pulse Rate Variability Analysis from Forehead and Finger PPG Signals *Physiol. Meas.* **40(2)** 025007.

Bailón R, Laouini G, Grao C, Orini M, Laguna P and Meste O 2011 The Integral Pulse Frequency Modulation with Time-Varying Threshold: Application to Heart Rate Variability Analysis during Exercise Stress Testing *IEEE Trans. Biomed. Eng.* **58(3)** 642–52.

Sun S, Peeters W H, Bezemer R, Long X, Paulussen I, Aarts R M and Noordergraaf G J 2019 Finger and forehead photoplethysmography-derived pulse-pressure variation and the benefits of baseline correction *J. Clin. Monit. Comput* **33(1)** 65–75.

Javed F, Middleton P M, Malouf P, Chan G S H, Savkin A V, Lovell N H, Steel E and Mackie J 2010 Frequency spectrum analysis of finger photoplethysmographic waveform variability during haemodialysis *Physiol. Meas.* **31(9)** 1203–16.

De Meersman, Ronald E 1993 Aging as a modulator of respiratory sinus arrhythmia *J. Gerontol.* **48(2)** B74–8.

Hirsch J A and Bishop B 1981 Respiratory sinus arrhythmia in humans: how breathing pattern modulates heart rate *Am. J. Physiol.* **241(4)** H620–9.

Lázaro J, Bailón R, Laguna P, Nam Y, Chon K and Gil E 2014b Respiratory rate influence in the resulting magnitude of pulse photoplethysmogram derived respiration signals *Proc. XLI Int. Conf. Comp. Card.* 289–92.

Pfurtscheller G, Schwarz G and Schwerdtfeger A 2018 Heart rate variability and impact of central pacemaker on cardiac activity *Clin. Neurophysiol.* **129(10)** 2188–90.